Appendix

Climate-driven legacies in simulated microbial communities alter litter decomposition rates

Bin Wang[1,2] and Steven Allison[2,3]

1 Environmental Sciences Division, Oak Ridge National Laboratory, Oak Ridge, TN 37830 USA

2 Department of Ecology and Evolutionary Biology, University of California, Irvine, CA 92697 USA

3 Department of Earth System Science, University of California, Irvine, CA 92697 USA

1. Gradient information

All five sites (**Supporting Fig. 1**) are located on granitic parent material and experience Mediterranean precipitation patterns (cool, wet winters; hot, dry summers) with different vegetation communities. The desert is dominated by desert perennials and annuals. The scrubland is dominated by pinyon pine, juniper, and desert perennials and annuals. The grassland is dominated by annual grasses and forbs, particularly *Bromus* and *Avena spp*. The pine-oak forest is dominated by pines as well as evergreen and deciduous oak. The subalpine site is dominated by lodgepole and limber pine.

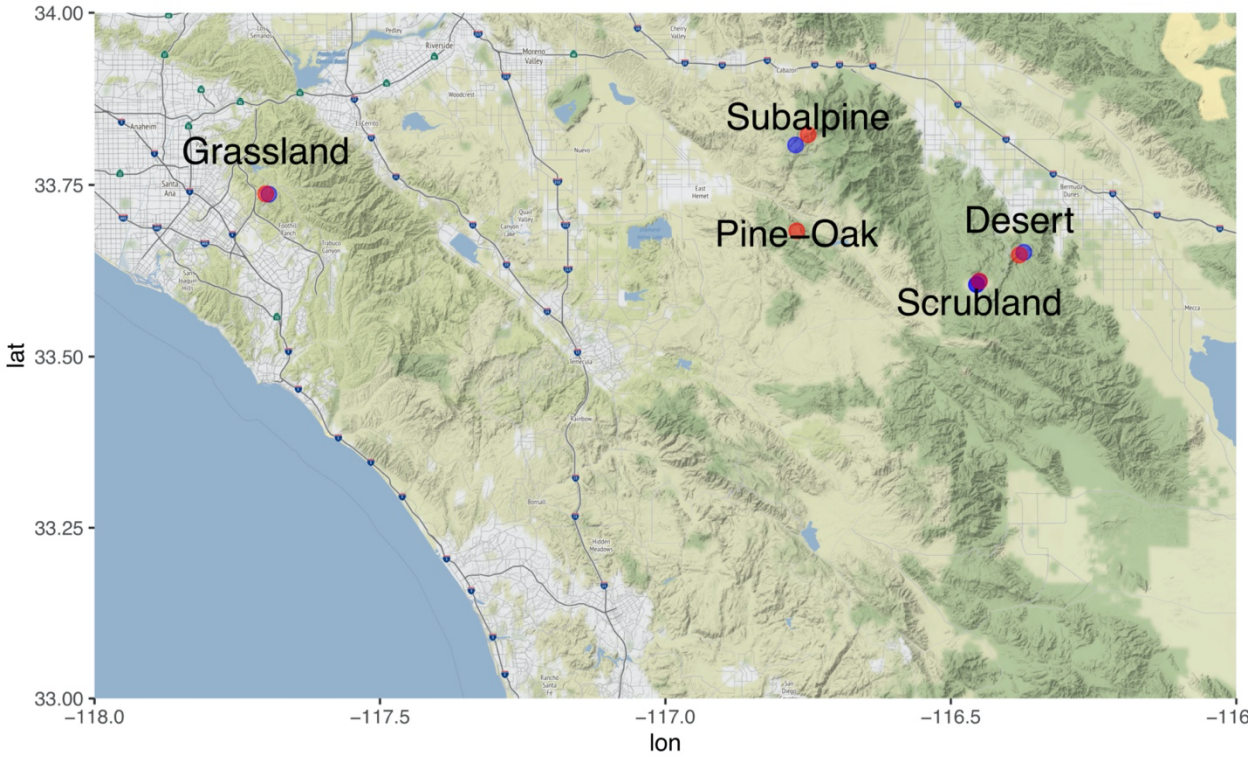

Supporting Fig. 1 Location of the five sites in Southern California, US. Blue dots are nearby eddy covariance flux tower sites (see https://www.ess.uci.edu/~california/). TAP (Total Annual Precipitation; mm) = [213.5, 428.4, 569.4, 1415.8, 1376.5], while MAT (Mean Annual Temperature; °C) = [22.8, 15.6, 16.4, 12.3, 10.3] from desert through subalpine.

2. DEMENTpy forcing

2.1 Average forcing

One-year average forcing was approximated by leveraging the litter water potential data available at the grassland site, near Loma Ridge, California (**Allison and Goulden 2017**) and field soil temperature measurements across the gradient (**Glassman et al. 2018**). Water potential (ψ_{site}; MPa) of the other four sites was derived by scaling the grassland site daily water potential ($\psi_{grassland}$) from 2011 (representative of typical annual conditions before the subsequent

megadrought in California) with Total Annual Precipitation (TAP; *mm*) and Mean Annual Temperature (MAT; °C) at each site following:

$$\psi_{site} = [1 + \ln\left(\frac{TAPgrassland}{TAPsite}\right)\frac{MATsite}{MATgrassland}]\psi_{grassland}$$

Soil temperatures at a sub-daily time step across the gradient at each of the five sites were measured. From these field measurements, daily soil temperature was derived by averaging all measurements in each day. Details with regards to the measurement method, pre-, and post-processing are documented in **Glassman et al. (2018)**. These data are openly accessible at https://github.com/stevenallison/UCIClimateExperiment/tree/master/updatednames. Data were further smoothed to obtain the average forcing dataset (**Supporting Fig.2)**.

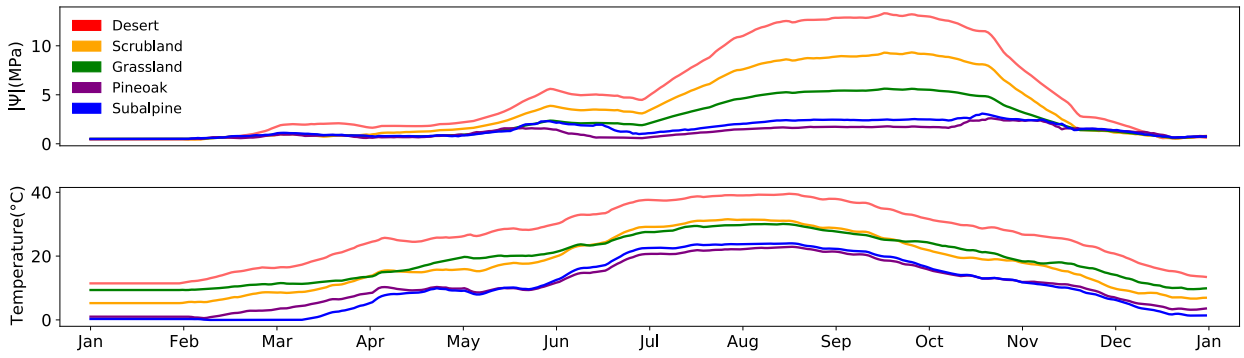

Supporting Fig. 2 Average forcing of temperature and water potential. This forcing was recycled to equilibrate microbiomes at different sites.

2.2 Actual forcing

Actual forcing follows the field transplant timeline (**Glassman et al. 2018**) to derive forcing for 2015-2019. Daily soil surface temperature (°C) was from the Daymet (version 4; **Thornton et al. 2020**) daily temperature product. Based on a machine learning framework, the estimation of water potential fully leveraged all data available at the grassland site, near Loma Ridge, California (2011-2013) including daily precipitation, field measurement of daily soil surface temperature, and daily water potential derived from fuel moisture sensors (**Allison and Goulden 2017**) to train a simple linear model. This trained model was then used to derive water potential for each of the five sites from daily precipitation and air temperature data of 2015-2019 accessed from Daymet. The derived forcing is plotted in **Supporting Fig.3**.

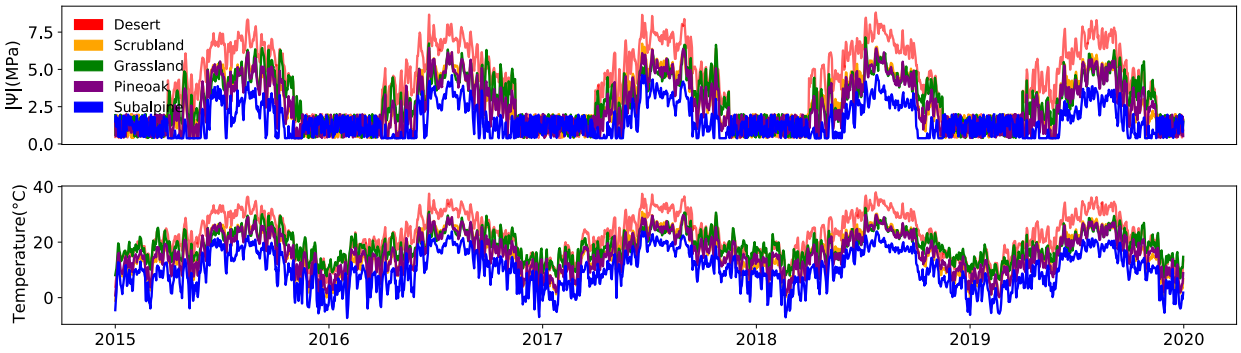

Supporting Fig. 3 Actual forcing from 2015 to 2019. Note that year 2015 was used after the 3-year spin-up but before transplant.

Table A1 Microbial and enzyme parameters and their values

Parameter	Value	Unit	Note
max_size_b	2	mg cm^{-3}	C quota threshold for bacterial cell division
Cfrac_b	0.825	mg mg^{-1}	Bacterial C fraction
Nfrac_b	0.16	mg mg^{-1}	Bacterial N fraction
Pfrac_b	0.015	mg mg^{-1}	Bacterial P fraction
Crange	0.09	mg mg^{-1}	Tolerance on C fraction
Nrange	0.04	mg mg^{-1}	Tolerance on N fraction
Prange	0.005	mg mg^{-1}	Tolerance on P fraction
C_min	0.086	mg cm^{-3}	Threshold C concentration for cell death
N_min	0.012	mg cm^{-3}	Threshold P concentration for cell death
P_min	0.002	mg cm^{-3}	Threshold C concentration for cell death
Uptake_C_cost_min	0.01	transporter mg^{-1} biomass C	Minimum per enzyme C cost as a fraction of uptake
Uptake_C_cost_max	0.1	transporter mg^{-1} biomass C	Maximum per enzyme C cost as a fraction of uptake
Uptake_Maint_cost	0.01	mg C $transporter^{-1}$ day^{-1}	Respiration cost of uptake transporters
Enz_per_taxon_min	0		Minimum number of enzymes a taxon can produce
Enz_per_taxon_max	40		Maximum number of enzymes a taxon can produce
Enz_Prod_min	0.00001	mg C mg^{-1} day^{-1}	Minimum per enzyme production cost as a fraction of C uptake rate
Enz_Prod_max	0.0001	mg C mg^{-1} day^{-1}	Maximum per enzyme production cost as a fraction of C uptake rate
Constit_Prod_min	0.00001	mg C mg^{-1} day^{-1}	Minimum per enzyme production cost as a fraction of biomass C
Constit_Prod_max	0.0001	mg C mg^{-1} day^{-1}	Maximum per enzyme production cost as a fraction of biomass C
Osmo_per_taxon_min	1		Minimum number of osmolyte a taxon can produce
Osmo_per_taxon_max	1		Maximum number of osmolyte a taxon can produce
Osmo_Consti_Prod_min	0.0000001	mg C mg^{-1} day^{-1}	Minimum per osmolyte production cost as a fraction of biomass C
Osmo_Consti_Prod_max	0.000001	mg C mg^{-1} day^{-1}	Maximum per osmolyte production cost as a fraction of biomass C
Osmo_Induci_Prod_min	0.01	mg C mg^{-1} day^{-1}	Minimum per osmolyte production cost as a fraction of C uptake rate
Osmo_Induci_Prod_max	0.1	mg C mg^{-1} day^{-1}	Maximum per osmolyte production cost as a fraction of C uptake rate
CUE_ref	0.5	mg mg^{-1}	Growth efficiency at the reference temperature
CUE_temp	-0.005	mg mg^{-1}	Growth efficiency change with enzyme investment
death_rate_bac	0.001		Bacterial death rate
basal_bac	10		Bacterial basal death probability
wp_th	-2.00	MPa	Water potential threshold at which osmolyte is induced
alpha	0.01	mg C mg^{-1} day^{-1}	Osmolyte production change with water potential
Vmax0_min	5	mg substrate mg^{-1} enzyme day^{-1}	Minimum Vmax for enzyme
Vmax0_max	50	mg substrate mg^{-1} enzyme day^{-1}	Maximum Vmax for enzyme

Uptake_Vmax0_min	1	mg substrate mg^{-1} substrate day^{-1}	Minimum uptake Vmax
Uptake_Vmax0_max	10	mg substrate mg^{-1} substrate day^{-1}	Maximum uptake Vmax
Uptake_Ea_min	35	kj mol^{-1}	Minimum activation energy for uptake
Uptake_Ea_max	35	kj mol^{-1}	Maximum activation energy for uptake
Km_min	0.01	mg cm^{-3}	Minimum Km
Uptake_Km_min	0.001	mg cm^{-3}	Minimum uptake Km
Vmax_Km	1	mg enzyme day cm^{-3}	Slope for Km-Vmax relationship
Vmax_Km_int	0	mg cm^{-3}	Intercept for Km-Vmax relationship
Uptake_Vmax_Km	0.2	mg biomass day cm^{-3}	Slope for uptake Km-Vmax relationship
Uptake_Vmax_Km_int	0	mg cm^{-3}	Intercept for uptake Km-Vmax relationship
Specif_factor	1		Enzyme efficiency-specificity

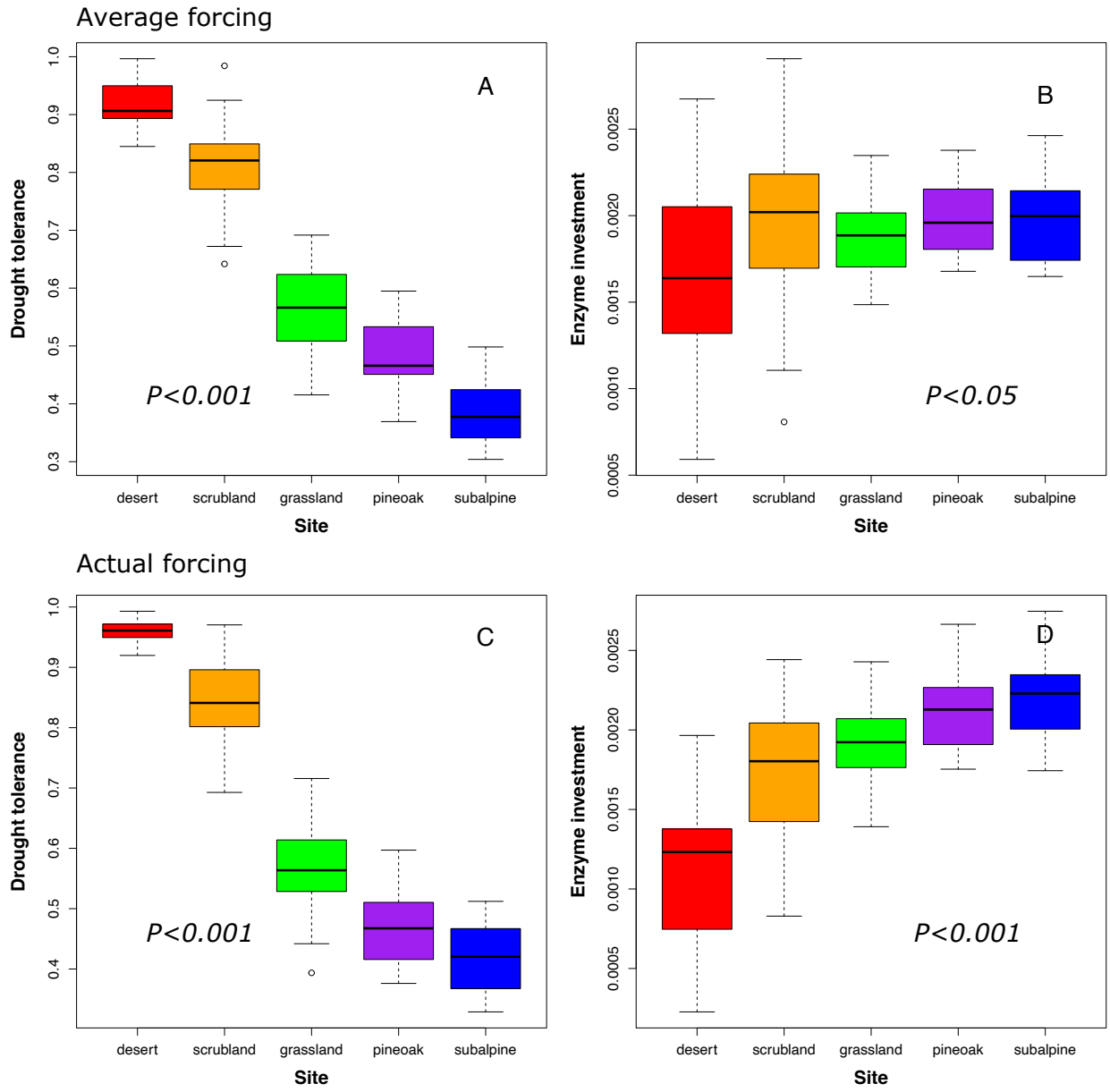

Supporting Fig. 4 Microbial community traits (drought tolerance and enzyme investment; n=20) at the five sites across the gradient before transplant after spin-up under average forcing (A, B) and actual forcing (C, D). The p values are derived from one-way ANOVA.

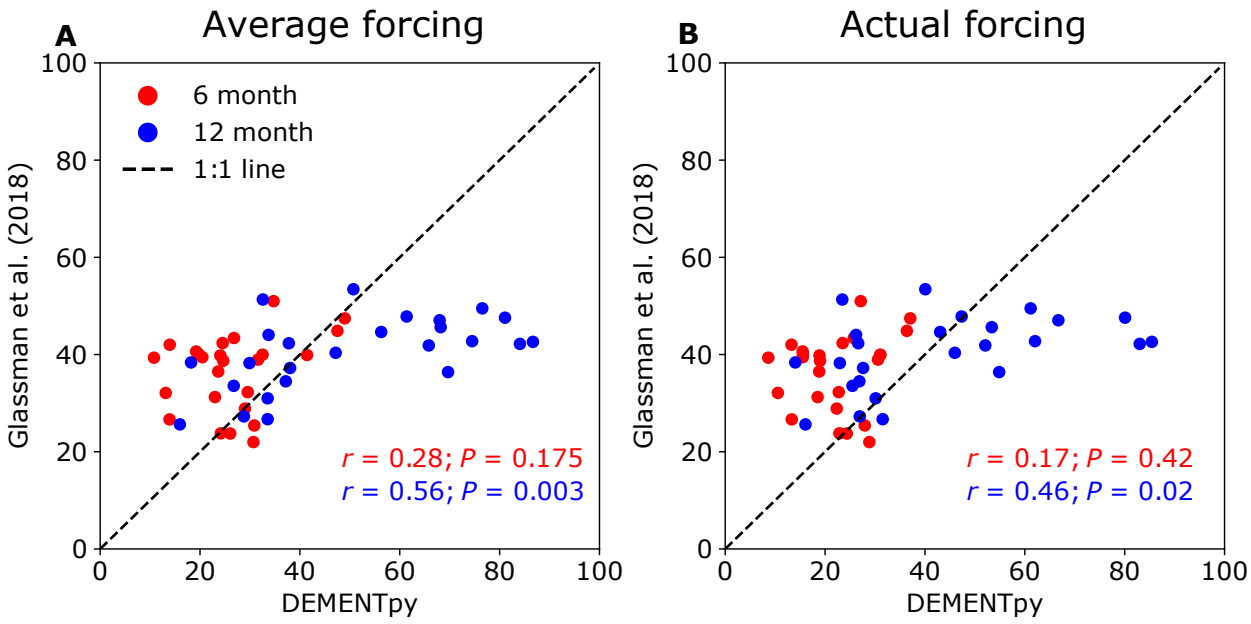

Supporting Fig. 5. Simulated litter mass loss (%) versus empirical results by Glassman et al. (2018) under average (A) and actual forcing (B). Red and blue points are percent mass loss by 6 months and 12 months, respectively, after transplant across the gradient. Pearson correlation is shown for both 6- and 12-month data. The Glassman et al. mass loss data are accessible at https://github.com/stevenallison/UCIClimateExperiment.

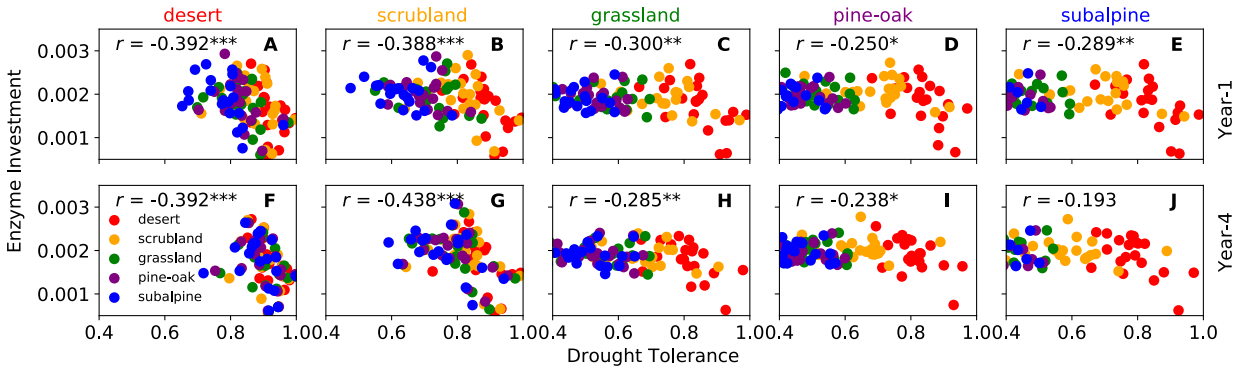

Supporting Fig. 6 Correlations between enzyme investment and drought tolerance across the gradient. Significance code: $P < 0.001$(***), $P < 0.01$(**), and $P < 0.05$ (*). Panels correspond to sites and symbols correspond to community origin.

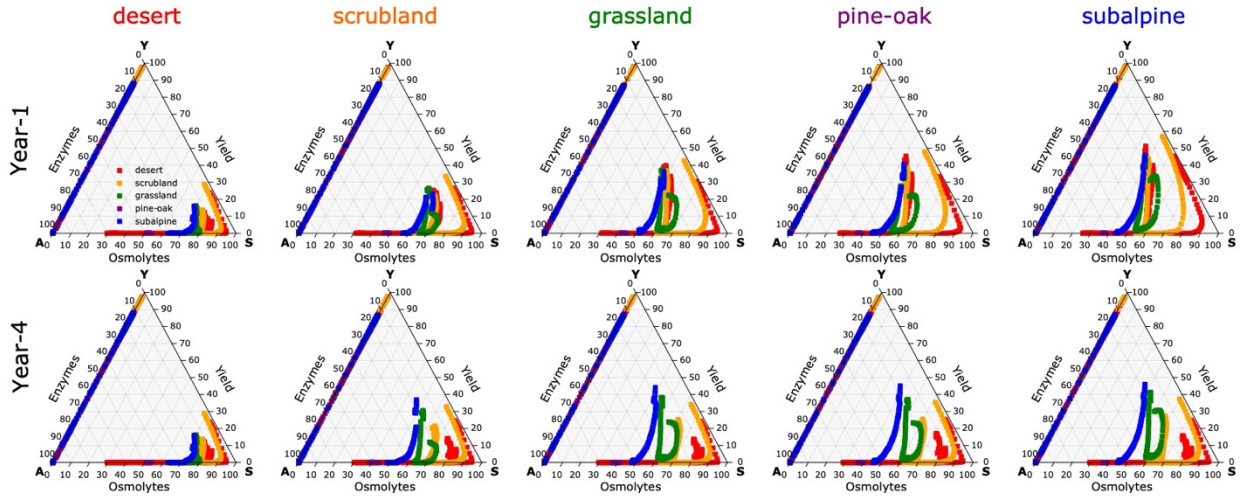

Supporting Fig. 7 Ternary plots of community allocation among enzymes, osmolytes, and yield over the whole year. Yield, enzymes, and osmolytes correspond to Y (Yield), A (resource Acquisition), and S (Stress), respectively. Points along the Y-A edge are low in osmolyte production in the wet season. At the desert site, from the 1st year through the 4th year, resource allocation among enzymes, osmolytes, and yield displayed little change (i.e., unchanged correlation strength); communities all had more allocation to osmolyte production by only differentiating along the A-S edge (i.e., stronger correlation between drought tolerance and enzyme investment as shown in **Supporting Fig. 6A, F**). At the grassland site, from the 1st through the 4th year, the allocation pattern changed, with communities having higher yield (i.e., lower correlation strength; **Supporting Fig. 6C, H**) and communities differentiating not only along the A-S dimension (i.e., correlation strength lower than the desert site). At the subalpine site, allocation by communities became more yield-driven from the 1st year through the 4th year (i.e., uncorrelated drought tolerance and enzyme investment as shown in **Supporting Fig. 6E, J**).